The Abdus Salam International Centre for Theoretical Physics

United Nations Educational, Scientific and Cultural Organization

IAEA International Atomic Energy Agency

1856-43

2007 Summer College on Plasma Physics

30 July - 24 August, 2007

Nonlinear rapid cooling of relativistic electrons under cosmic equipartition plasma conditions

R. Schlickeiser

Ruhr University
Bochum, Germany

Nonlinear rapid cooling of relativistic electrons under cosmic equipartition plasma conditions

Reinhard Schlickeiser
Institut für Theoretische Physik
Lehrstuhl IV: Weltraum- und Astrophysik
Ruhr-Universität Bochum, Germany

August 23, 2007

Topics:

1. Introduction
2. Evolution of radiating electrons under equipartition conditions
3. Instantaneous injection of monoenergetic electrons
4. Optically thin synchrotron intensities, light curves and fluences – Monoenergetic injection
5. Steady-state solution for monoenergetic injection
6. Instantaneous power law injection
7. Steady-state solution for power law injection
8. Summary and conclusions

References:

Nonlinear radiative cooling of relativistic particles under equipartition conditions I. Instantaneous monoenergetic injection; R. Schlickeiser and I. Lerche, 2007, Astron. Astrophys., submitted

Nonlinear radiative cooling of relativistic particles under equipartition conditions II. Instantaneous power law injection; R. Schlickeiser and I. Lerche, 2007, Astron. Astrophys., submitted

1. Introduction

- Increasing evidence for the coupling of the physical processes for particle acceleration and magnetic field generation in relativistic outflow sources (jets of active galactic nuclei, gamma-ray bursts):

  1) Numerical modelling of observed blazar SEDs (e.g. Dermer and RS 2002, Böttcher and Chang 2002) provides best agreement if equipartition conditions are taken between energy densities of magnetic fields ($U_B = B^2/8\pi$) and relativistic electrons $U_e(t) = \int_0^\infty dp \gamma m_e c^2 N(p,t)$:

  $$e_B = U_B(t)/U_e(t) = \text{const.}$$

  2) Similar equipartition assumption is made in nonthermal radiation models for gamma-ray burst afterglows (Meszaros and Rees 1997, Frail et al. 2000): fixed fraction ϵ_e of blast wave energy E_0 goes into accelerating a power law distribution of electrons above lower threshold γ_m, fixed fraction ϵ_B of blast wave energy E_0 is in magnetic field. Partition ratio then is $e_B = \epsilon_B/\epsilon_e \neq 1$.

- Central role played by Weibel-type instabilities generating aperiodic magnetic fluctuations $\delta B \propto \exp(\imath \vec{k} \cdot \vec{x} + \Gamma t), \quad \omega_R = 0$

  Free energy reservoir for instability = kinetic relativistic outflow energy

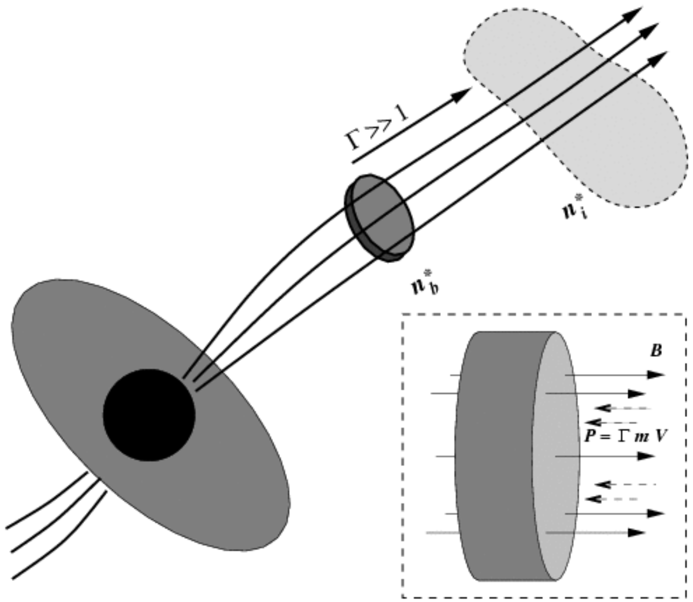

- These instabilities are best known in unmagnetized ($B_0 = 0$) plasmas but also occur in weakly magnetized ($B_0 < B_c$) plasmas (see talk by M. Dieckmann). The instabilities are suppressed in strongly magnetized plasmas ($B_0 > B_c$).

- counterstream plasma instabilities of dense outflow plasma in dilute ambient gas $n_b^* >> n_i^*$ ("relativistic pick-up model")
- $B_0 = 0$: interstellar p^+, e^-, neutrals enter as weak beam, beam excites aperiodic magnetic fluctuations (δB) perpendicular to counterstream direction that isotropise incoming p^+, e^- after time t_s, i.e. **pick-up of interstellar ions and electrons in outflow**

consequence 1: outflow picks up interstellar p^+ and e^- with

$$E_{p,\max} = \Gamma m_p c^2 = 100\Gamma_{100} \text{ GeV}$$

$$E_{e,\max} = \Gamma m_e c^2 = 0.05\Gamma_{100} \text{ GeV}$$

primary energy output at TeV energies in lab frame:

in $p^+ - e^-$ outflows $E^*_{\gamma,\max} = 20\Gamma^2_{100}$ TeV

in pair outflows $E^*_{\gamma,\max} = 0.01\Gamma^2_{100}$ TeV

consequence 2: equipartition conditions

Note: we use ultrarelativistic approximation in source frame $\gamma \simeq p/mc$

2. Evolution of radiating electrons under equipartition conditions

Use Kardashev (1962) approach for time evolution of the volume-averaged relativistic electron population inside the radiating source ($n(\gamma,t)$ is volume-averaged differential number density)

$$\frac{\partial n(\gamma,t)}{\partial t} - \frac{\partial}{\partial \gamma}\left[\dot{\gamma} n(\gamma,t)\right] = Q(\gamma,t)$$

subject to injection $Q(\gamma,t)$ and synchrotron radiation losses

$$\dot{\gamma} = D_0\gamma^2, \quad D_0 = \frac{4}{3}\frac{c\sigma_T}{m_e c^2}U_B = 2.66\cdot 10^{-14}\left[\frac{U_B}{m_e c^2}\right]\ s^{-1}$$

2.1. Linear cooling

For constant energy density U_B kinetic equation is linear with solution:

$$n_L(\gamma,t) = \int_0^\infty d\gamma_0 \int_{-\infty}^\infty dt_0 Q(\gamma_0,t_0)G(\gamma,\gamma_0,t,t_0)$$

with Green's function

$$G(\gamma,\gamma_0,t,t_0) = H[\gamma_0-\gamma]H[t-t_0]\delta(\gamma - \frac{\gamma_0}{1+D_0\gamma_0 t})$$

($H[x]$ denotes Heaviside's step function)

2.2. Nonlinear cooling

(a) under partition conditions, $U_B = e_B m_e c^2 \int_0^\infty d\gamma \gamma n(\gamma, t)$, the synchrotron cooling of relativistic electrons depends on the kinetic energy density of the radiating particles,

$$\dot{\gamma} = A_0 \gamma^2 \int_0^\infty d\gamma \gamma n(\gamma, t), \quad A_0 = \frac{4}{3} c \sigma_T e_B$$

(b) moreover the magnetic field strength $B(t) = \sqrt{8\pi e_B U_e(t)}$ is time-dependent, changing not only the temporal behaviour of the relativistic electron energy spectrum but, additionally, modifying the synchrotron photon emissivity.
As a consequence of (1), the evolution of relativistic electron energy spectra exhibits $nonlinear$ behaviour because the cooling of an individual electron is stronger with a larger kinetic energy density of the whole electron population.
Kinetic equation (1) then becomes nonlinear

$$\frac{\partial n}{\partial t} - A_0 [\int_0^\infty d\gamma \gamma n] \frac{\partial}{\partial \gamma} (\gamma^2 n) = Q(\gamma, t) \tag{2}$$

Method of Green's function solution does not work. Have to do each injection case separately.

3. Instantaneous injection of monoenergetic electrons

Injection rate: $Q(\gamma, t) = q_0 \delta(\gamma - \gamma_0)\delta(t)$

3.1. Linear solution:

$$n_L(\gamma, t) = q_0 H[\gamma_0 - \gamma]\delta\left(\gamma - \gamma_L(t)\right), \quad \gamma_L(t) = \frac{\gamma_0}{1 + D_0\gamma_0 t}$$

An electron starting with Lorentz factor γ_0 has cooled to the Lorentz factor γ_L at later times. The half-life time is

$$t^L_{1/2} = \frac{1}{D_0\gamma_0} = \frac{3.76 \cdot 10^{13}}{\gamma_0}\left[\frac{4.54\ \mathrm{mG}}{B}\right]^2 \quad \mathrm{s}$$

depends inversely on the initial Lorentz factor and the magnetic field strength but not on the injection rate q_0.

3.2. Nonlinear solution:

$$n_{NL}(\gamma,t) = q_0 H[\gamma_0 - \gamma]\delta\left(\gamma - \gamma_{NL}(t)\right), \quad \gamma_{NL}(t) = \frac{\gamma_0}{\sqrt{1+2A_0 q_0 t\gamma_0^2}}$$

implies modified synchrotron energy loss rate in equipartition conditions

$$\dot{\gamma}_{NL} = D_0 m_e c^2 \frac{U_B(0)}{U_e(0)} \gamma_{NL}^3$$

Here, an electron starting with Lorentz factor γ_0 cools to the Lorentz factor γ_{NL} at later times but γ_{NL} differs substantially from the linear Lorentz factor $\gamma_L(t)$. Now half-life time, $t_{1/2}^{NL}$, is

$$t_{1/2}^{NL} = \frac{3}{2A_0 q_0 \gamma_0^2} = \frac{9}{8c\sigma_T e_B q_0 \gamma_0^2} = 5.64 \cdot 10^{13} e_B^{-1} [q_0/\mathrm{cm}^{-3}]^{-1} \gamma_0^{-2} \quad \mathrm{s}$$

which depends on the initial kinetic energy of injected electrons (proportional to $q_0\gamma_0$), and it depends differently than in the linear case on the initial electron Lorentz factor (inversely quadratic instead of inversely linear) and also inversely on the value of the injection rate q_0.
The more electrons are injected, the quicker each electron cools under equipartition requirements. **Such a collective behaviour is new and completely different from the linear case.**

3.3. Timescale comparison:

The ratio of nonlinear to linear half-life time is much smaller than unity provided

$$q_0\gamma_0 > \frac{3}{2e_B}\left[\frac{B}{4.54\ \mathrm{mG}}\right]^2$$

Fulfilled in GRB sources and blazars:
Modelling of blazar flaring (e.g. Dermer and Schlickeiser 1992, 2002): about $q_0 \simeq 10^5$ electrons per cm^{-3} with Lorentz factors $\gamma_0 \simeq 10^7$ are injected in sources with several Gauss ($B \simeq 10$ G) magnetic fields, much below the initial equipartition field strength. The nonlinear half-life is then more than four orders of magnitude shorter than the standard linear half-life.
$\rightarrow$ dramatic reduction of the intrinsic radiation loss times due to equipartition conditions. Agreement with the observed short time variability from flaring blazar jets, of order minutes as in PKS 2155-304 (Aharonian et al. 2007), of order seconds in GRBs, and of order days in case of the non-blazar radio galaxy M 87 (Aharonian et al. 2006).
It is easy to show that with assumed equipartition conditions $U_B(0) = q_0\gamma_0 m_e c^2 e_B$ the linear half-life time is comparable to the nonlinear half-life time, $t^L_{1/2} = (2/3)t^{NL}_{1/2}$.

4. Optically thin synchrotron intensities, light curves and fluences – Monoenergetic injection

For homogenous source of diameter L the optically thin synchrotron intensity is

$$I(\nu,t) = \frac{L}{4\pi}\int_0^\infty d\gamma\, n(\gamma,t)P(\nu,\gamma)$$

with synchrotron power

$$P(\nu,\gamma) = P_0\frac{\nu}{\gamma^2}CS\left[\frac{2\nu}{3\nu_0\gamma^2}\right]$$

with electron gyrofrequency $\nu_0 =$ and $CS(x) = x^{-2/3}/(0.869 + x^{1/3}e^x)$.

Normalized time coordinates: $x_L = t/t^L_{1/2}$, $x_{NL} = 3t/t^{NL}_{1/2}$

Normalized frequencies

$$f_L \equiv \frac{\nu}{\nu_L(t=0)} = \frac{\nu}{\frac{3}{2}\nu_0\gamma_0^2}, \quad f_{NL} \equiv \frac{\nu}{\nu_{NL}(t=0)} = \frac{\nu}{\frac{3}{2}c\sqrt{2e_B q_0 r_0/\pi}\gamma_0^{5/2}}$$

Combined variables: $s_L \equiv f_L(1+x_L)^2$, $s_{NL} = f_{NL}(1+x_{NL})^{5/4}$

4.1. Intensities

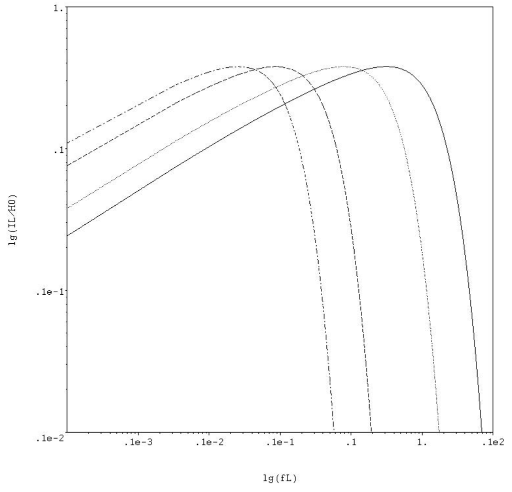

Figure 1: Linear synchrotron intensity at four different times

$$I_L(f_L, x_L) = H_0 s_L CS\,[s_L] \simeq$$

$$1.151 H_0 s_L^{1/3} = 1.151 H_0 f_L^{1/3}(1+x_L)^{2/3} \quad \text{for} \quad f_L(1+x_L)^2 << 0.282$$

$$H_0 \exp(-s_L) = H_0 \exp(-f_L(1+x_L)^2) \quad \text{for} \quad f_L(1+x_L)^2 >> 0.282$$

Maximum intensity at the frequency $f_{L,max} = 0.282/(1+x_L)^2$, which decreases $\propto 0.282 x_L^{-2}$ for large times $x_L >> 1$. However, the maximum intensity is independent of time.

Introduction
Evolution of . . .
Instantaneous . . .
Optically thin . . .
Steady-state . . .
Instantaneous . . .
Steady-state . . .
Summary and . . .

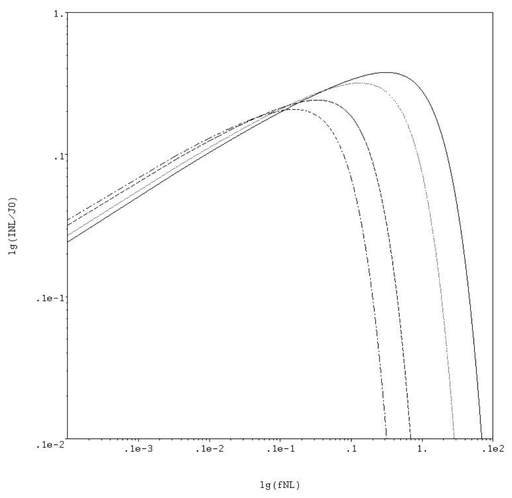

Figure 2: Nonlinear synchrotron intensity at four different times

$$I_{NL}(f_{NL}, x_{NL}) = \frac{J_0}{(1+x_{NL})^{1/4}} s_{NL} CS\left[s_{NL}\right] \simeq$$

$$\frac{J_0}{(1+x_{NL})^{1/4}} 1.151 f_{NL}^{1/3} (1+x_{NL})^{5/12} \quad \text{for} \quad f_{NL}(1+x_{NL})^{5/4} << 0.282$$

$$\frac{J_0}{(1+x_{NL})^{1/4}} \exp(-f_{NL}(1+x_{NL})^{5/4}) \quad \text{for} \quad f_{NL}(1+x_{NL})^{5/4} >> 0.282$$

Maximum intensity at $f_{NL,max} = 0.282/(1+x_{NL})^{5/4}$, which decreases $\propto 0.282 x_{NL}^{-5/4}$ at large times. Also the maximum intensity itself decreases as $\propto x_{NL}^{-1/4}$ with increasing time.

Introduction
Evolution of . . .
Instantaneous . . .
Optically thin . . .
Steady-state . . .
Instantaneous . . .
Steady-state . . .
Summary and . . .

4.2. Light curves

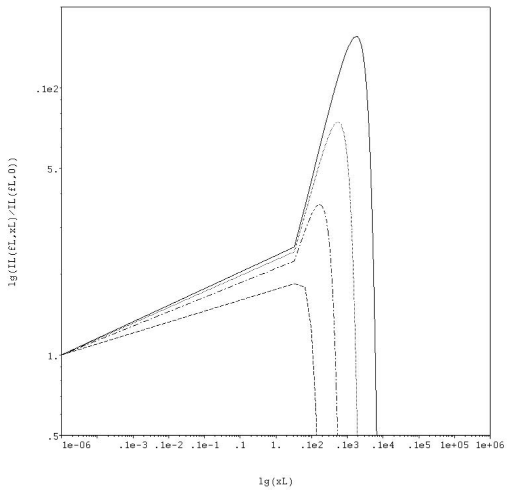

Figure 3: Linear synchrotron light curve at four different frequencies

At frequencies below $f_L << 0.282$ transition from a power law increase to a Gaussian decay at $x_L = 0.53/\sqrt{f_L}$:

$$\frac{I_L(x_L)}{I_L(x_L = 0)} \simeq (1 + x_L)^{2/3} \quad \text{for} \quad x_L << 0.53/f_L^{1/2}$$

$$\frac{I_L(x_L)}{I_L(x_L = 0)} \simeq \exp[-f_L(x_L^2 + 2x_L)] \quad \text{for} \quad x_L >> 0.53/f_L^{1/2}$$

The width of the Gaussian increases $\propto f_L^{-1/2}$ with decreasing frequency.

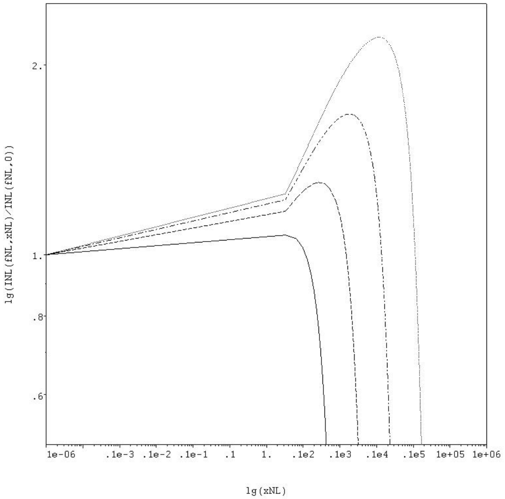

Figure 4: Nonlinear synchrotron light curve at four different frequencies

At frequencies below $f_{NL} << 0.282$, there is a transition from a weaker power law increase to a non-Gaussian decay at $x_{NL} = (0.282/f_L)^{4/5}$

$$\frac{I_{NL}(x_{NL})}{I_{NL}(x_{NL}=0)} \simeq (1+x_{NL})^{1/6} \quad \text{for} \quad x_{NL} << 0.363 f_{NL}^{-0.8}$$

$$\frac{I_{NL}(x_{NL})}{I_{NL}(x_{NL}=0)} \simeq x_{NL}^{-1/4} \exp[-f_{NL} x_{NL}^{5/4}] \quad \text{for} \quad x_{NL} >> 0.363 f_{NL}^{-0.8}$$

Introduction
Evolution of . . .
Instantaneous . . .
Optically thin . . .
Steady-state . . .
Instantaneous . . .
Steady-state . . .
Summary and . . .

4.3. Synchrotron fluences

Time-integrated synchrotron fluence $F(f) = \int_0^\infty dt\, I(f,t)$:

At large normalized frequencies $f_L >> 1$ and $f_{NL} >> 1$ both fluences exhibit the same exponential cut-off

$$F_L(f_L >> 1) \simeq \frac{H_0 t^L_{1/2}}{2} f_L^{-1} e^{-f_L}$$

$$F_{NL}(f_{NL} >> 1) \simeq \frac{4 J_0 t^{NL}_{1/2}}{15} f_{NL}^{-1} e^{-f_{NL}}$$

At small normalized frequencies the nonlinear fluence shows a steeper (by $\Delta\alpha = 0.1$) power law behaviour ($\propto f_{NL}^{-0.6}$) than the linear fluence ($\propto f_L^{-0.5}$)

$$F_L(f_L << 1) \simeq \frac{H_0 t^L_{1/2} c_0}{2} f_L^{-1/2}$$

$$F_{NL}(f_{NL} << 1) \simeq \frac{4 J_0 c_1 t^{NL}_{1/2}}{15} f_{NL}^{-3/5}$$

5. Steady-state solution for monoenergetic injection

Differences also in steady-state solution for monoenergetic injection $Q(\gamma) = Q_0\delta(\gamma - \gamma_0)$, $\gamma_0 >> 1$:

Linear solution $N_L(\gamma) = \frac{Q_0}{D_0}\gamma^{-1}[\gamma^2 - 1]^{-1/2}H[\gamma_0 - \gamma]$

Nonlinear solution $N_{NL}(\gamma) = \sqrt{\frac{Q_0}{A_0[\ln\gamma_0 + (\pi/2)]}}\gamma^{-1}[\gamma^2 - 1]^{-1/2}H[\gamma_0 - \gamma]$

Identical energy dependence but different dependences on injection rate Q_0 and initial Lorentz factor γ_0.

6. Instantaneous power law injection

Injection rate: $Q(\gamma, t) = q_0 \gamma^{-s} \delta(t)$ for $1 << \gamma_1 \leq \gamma \leq \gamma_2$

6.1. Linear solution:

quenched cooled power law

$$n_L(\gamma, t) = q_0 \gamma^{-s} [1 - D_0 \gamma t]^{s-2}$$

for $\gamma_1(t) \leq \gamma \leq \gamma_2(t)$ with

$$\gamma_1(t) = \frac{\gamma_1}{1 + D_0 \gamma_1 t}, \quad \gamma_2(t) = \frac{\gamma_2}{1 + D_0 \gamma_2 t}$$

Exhibits Kardashev-pile up for values $s < 2$.

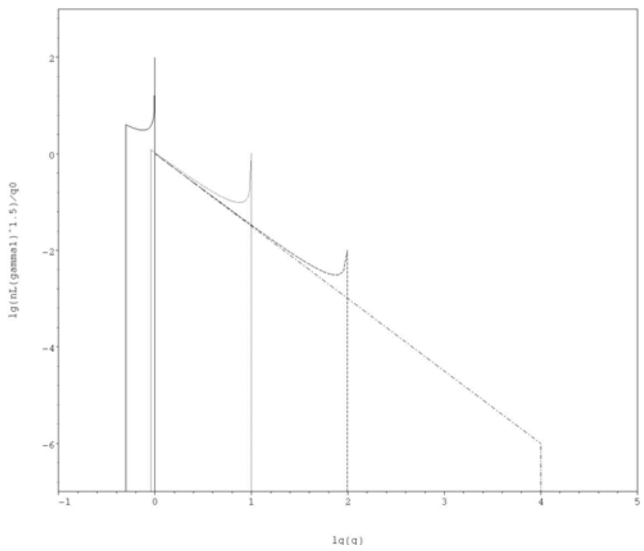

Figure 5: Electron distribution function $n_L \gamma_1^{3/2}/q_0$ as a function of the normalized Lorentz factor $g = \gamma/\gamma_1$ for $s = 1.5$ and $g_2 = \gamma_2/\gamma_1 = 10^4$ in the linear cooling case at different times $\tau = t/t_M = 0$ (dotted-dashed curve), 10^{-2} (dashed curve), 0.1 (thin full curve) and 1 (thick full curve). Here $t_M = D_0\gamma_1$.

6.2. Nonlinear solution:

$$n_{NL}(\gamma,t) = q_0\gamma^{-s}[1-\gamma T(y)]^{s-2}H[\frac{\gamma_2}{1+\gamma_2 T(y)}-\gamma]H[\gamma-\frac{\gamma_1}{1+\gamma_1 T(y)}]$$

Variable $T(y)$ is related to the time $y = A_0 t$ through the first-order nonlinear differential equation ($x_1 = 1/\gamma_1,\ \ x_2 = 1/\gamma_2$)

$$T^{2-s}\frac{dT}{dy} = q_0\int_{x_2/T}^{x_1/T} dv\frac{v^{s-2}}{v+1}$$

This nonlinear differential equation can be solved approximately in the small time ($T \le x_2 << x_1$), the intermediate time ($x_2 \le T \le x_1$), and the late time ($x_2 << x_1 \le T$) limits, respectively.

For flat spectral index values $1 < s < 2$ we obtain approximately

$$T(0 \le y \le y_2, s < 2) \simeq \frac{q_0}{s-2} x_2^{s-2} y$$

$$T(y_2 \le y \le y_1, s < 2) \simeq \left[\frac{3-s}{(2-s)(s-1)} q_0 y - \frac{2(2-s)}{s-1} x_2^{3-s} \right]^{1/(3-s)}$$

$$T(y \ge y_1, s < 2) \simeq \left[\frac{2q_0}{s-1} x_1^{s-1} y + \frac{s-1}{3-s} x_1^2 - \frac{4(2-s)^2}{(3-s)(s-1)} x_2^{3-s} x_1^{s-1} \right]^{1/2}$$

with

$$y_1 = \frac{(2-s)(s-1)}{(3-s)q_0} \left[x_1^{3-s} + \frac{2(2-s)}{s-1} x_2^{3-s} \right], \quad y_2 = \frac{2-s}{q_0} x_2^{3-s}$$

For steep spectral index values $s > 2$ we find approximately

$$T(0 \le y \le y_3, s > 2) \simeq \frac{q_0}{s-2} x_1^{s-2} y$$

$$T(0 \le y \ge y_3, s > 2) \simeq \left[\frac{2q_0}{s-1} x_1^{s-1} y + \frac{3-s}{s-1} x_1^2 \right]^{1/2}$$

with

$$y_3 = \frac{s-2}{q_0} x_1^{3-s}$$

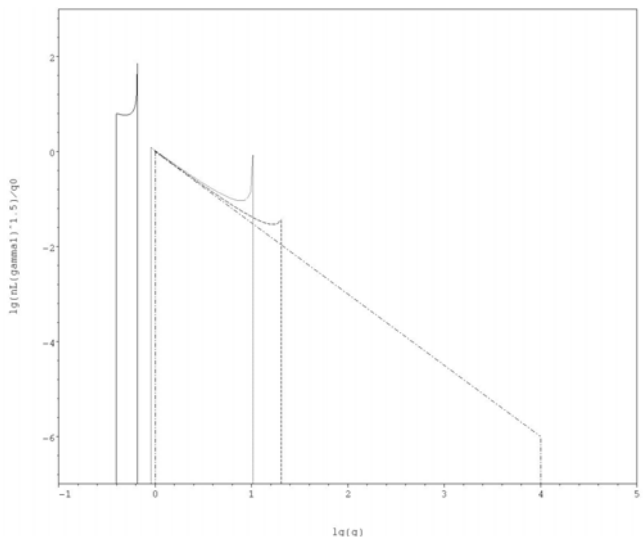

Figure 6: Electron distribution function $n_{NL}\gamma_1^{3/2}/q_0$ as a function of the normalized Lorentz factor $g = \gamma/\gamma_1$ for $s = 1.5$ and $g_2 = \gamma_2/\gamma_1 = 10^4$ in the nonlinear cooling case at different times $\tau = t/t_M = 0$ (dooted-dashed curve), 10^2 (dashed curve), 10^4 (thin full curve) and 10^6 (thick full curve).

6.3. Electron fluence distribution

Electron fluence $N(\gamma) = \int_0^\infty dt\, n(\gamma, t)$
For radiation processes not subject to equipartition conditions (inverse Compton scattering, relativistic bremsstrahlung) direct relation to corresponding radiation frequency fluences.

6.3.1. Linear fluence

$$N_L(\gamma \leq \gamma_1) = \frac{q_0}{D_0(s-1)}\gamma^{-2}\left[\gamma_1^{1-s} - \gamma_2^{1-s}\right]$$

$$N_L(\gamma_1 \leq \gamma \leq \gamma_2) = \frac{q_0}{D_0(s-1)}\gamma^{-(s+1)}\left[1 - (\frac{\gamma}{\gamma_2})^{s-1}\right]$$

This broken power law exhibits a spectral break by $\Delta s = s - 1$ at γ_1.

6.3.2. Nonlinear fluence for $s > 2$

$(g = \gamma/\gamma_1)$

$$N_{NL}(\gamma_1 < \gamma \leq \gamma_2, s > 2) = \frac{q_0 t_L \gamma_1}{s-1}\gamma^{-s-1}\left[1 - (\frac{\gamma}{\gamma_2})^{s-1}\right],$$

$$N_{NL}(\frac{\gamma_2}{1+\gamma_2} < \gamma \leq \gamma_1, s > 2) = \frac{q_0 t_L \gamma_1^{2-s}}{s-1}\gamma^{-2}\left[1 - (\frac{\gamma_1}{\gamma_2})^{s-1}\right],$$

$$N_{NL}(\frac{\gamma_1}{2} < \gamma \leq \frac{\gamma_2}{1+\gamma_2}, s > 2) = q_0 t_L \gamma^{-s}\Big[\frac{1}{g(s-1)}[g^{s-1} - (1-g)^{s-1}]$$

$$+\frac{s-1}{g^2(s-2)}\left[\frac{(1-g)^{s-1} - g^{s-1}g_2^{1-s}}{s-1} - \frac{(1-g)^s - g^s g_2^{-s}}{s}\right]\Big],$$

$$N_{NL}(\gamma \leq \frac{\gamma_1}{2}, s > 2) = \frac{q_0 t_L \gamma_1^{3-s}}{s-2}\gamma^{-3}\left(1 - (\frac{\gamma_1}{\gamma_2})^{s-1} - \frac{s-1}{s}\frac{\gamma}{\gamma_1}[1 - (\frac{\gamma_1}{\gamma_2})^s]\right)$$

For $\gamma \geq \gamma_1$ the nonlinear fluence distribution agrees with the linear steepened power law behaviour.
Different behaviour at lower Lorentz factors: much below the transition region $\gamma \simeq \gamma_1/2$ the nonlinear fluence approaches a power law $\propto \gamma^{-3}$ whose spectral index is larger by unity than in the linear case.
Consequently, we also obtain a broken power law behaviour for the nonlinear fluence, however with a smaller spectral break by $\Delta s = s-2$ around γ_1 than in the linear case.

6.3.3. Nonlinear fluence for $1 < s < 2$

At all energies $\gamma \leq \gamma_2/2$ we obtain an unbroken power law with spectral index 3 independent of the injected flat power law value $1 < s < 2$.

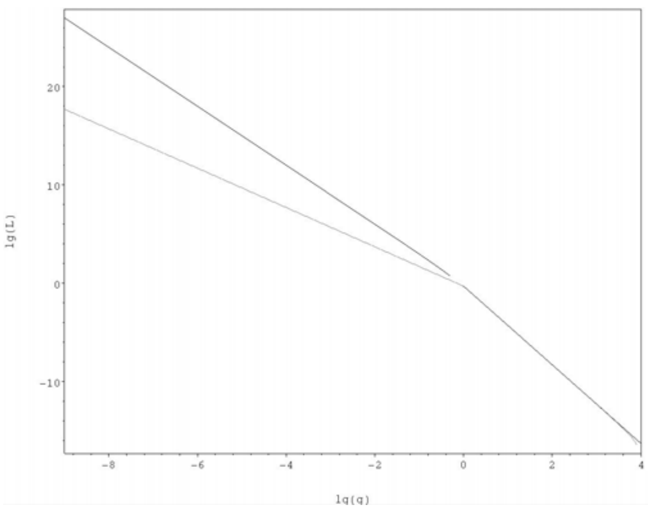

Figure 7: Linear (lower curve) and nonlinear (upper curve) electron fluence distribution function $N_L \gamma_1^3 / q_0 t_L$ as a function of the normalized Lorentz factor $g = \gamma/\gamma_1$ for $s = 3$ and $g_2 = \gamma_2/\gamma_1 = 10^4$ calculated for $t_L = (D_0 \gamma_1)^{-1}$.

Introduction
Evolution of . . .
Instantaneous . . .
Optically thin . . .
Steady-state . . .
Instantaneous . . .
Steady-state . . .
Summary and . . .

7. Steady-state solution for power law injection

Steady-state solution for power law injection $Q(\gamma) = Q_0\gamma^{-s}$, for $1 \le \gamma_1 \le \gamma \le \gamma_2$:

Linear solution

$$N_L(\gamma \le \gamma_1) = \frac{Q_0}{D_0(s-1)\gamma(\gamma^2-1)^{1/2}}\gamma_1^{1-s}[1-(\gamma_1/\gamma_2)^{s-1}]$$

$$N_L(\gamma_1 \le \gamma \le \gamma_2) = \frac{Q_0}{D_0(s-1)\gamma(\gamma^2-1)^{1/2}}\gamma^{1-s}[1-(\gamma/\gamma_2)^{s-1}]$$

Nonlinear solution

$$N_{NL}(\gamma \le \gamma_1) = \frac{Q_0^{1/2}\gamma_1^{(s-1)/2}}{[A_0(s-1)\ln\gamma_1]^{1/2}}\gamma^{-1}(\gamma^2-1)^{-1/2}[\gamma_1^{1-s}-\gamma_2^{1-s}]$$

$$N_{NL}(\gamma_1 \le \gamma \le \gamma_2) = \frac{Q_0^{1/2}\gamma_1^{(s-1)/2}}{[A_0(s-1)\ln\gamma_1]^{1/2}}\gamma^{-1}(\gamma^2-1)^{-1/2}[\gamma^{1-s}-\gamma_2^{1-s}]$$

Identical energy dependence but different dependence on injection rate Q_0 and on the initial cut-offs γ_1 and γ_2.

8. Summary and conclusions

- In powerful cosmic nonthermal radiation sources with dominant magnetic field self generation, the generation of magnetic fields at almost equipartition stength by relativistic plasma instabilities operates as fast as the acceleration or injection of ultra-high energy radiating electrons in these sources.

- The magnetic field strength then is time-dependent and adjusts itself to the actual energy density of the radiating electrons in these sources.

- As a consequence the synchrotron radiation cooling of individual relativistic electrons exhibits a nonlinear behaviour because of the dependence of the magnetic energy density on the particle energy density which itself decreases due to the time evolution of the electron number density.

- For different injection conditions we have solved this nonlinear kinetic equation for the intrinsic temporal evolution of relativistic electrons.

- In the case of instantaneous monoenergetic injection we calculate the corresponding optically thin synchrotron radiation intensity taking into account also the time-dependence of the magnetic field strength under equipartition conditions. The comparison with the synchrotron intensity from the standard solution of the linear kinetic equation shows significant differences both in the spectral distributions at different times and the synchrotron light curves at different frequencies. Spectral differences also occur in the frequency distribution of the linear and nonlinear synchrotron fluences.

- For power law injection the differential electron fluence as a function of electron energy differs from the linear electron fluence. For large spectral indices $s > 2$ of the injected power law the nonlinear fluence exhibits a weaker break at the lower injected electron cut-off γ_1 than the linear fluence. For small spectral indices $1 < s < 2$ the nonlinear fluence shows no break at all and approaches the $\propto \gamma^{-3}$ power law at all energies below $\gamma_2/2$.

- Under steady-state conditions for monoenergetic and power law injection the nonlinear and linear electron distribution functions exhibit the same dependence on the Lorentz factor of the electrons but their absolute values are different and depend differently on the injection rate Q_0.

- Predictions of spectral behaviour with energy, time and frequency provide tests for the presence or absence of linear or nonlinear cooling in flaring nonthermal sources.

- Hadrons are also subject to nonlinear synchrotron cooling in large magnetic field values, exactly what is expected under partition conditions. Offers potential method to test for hadron-induced radiation processes.

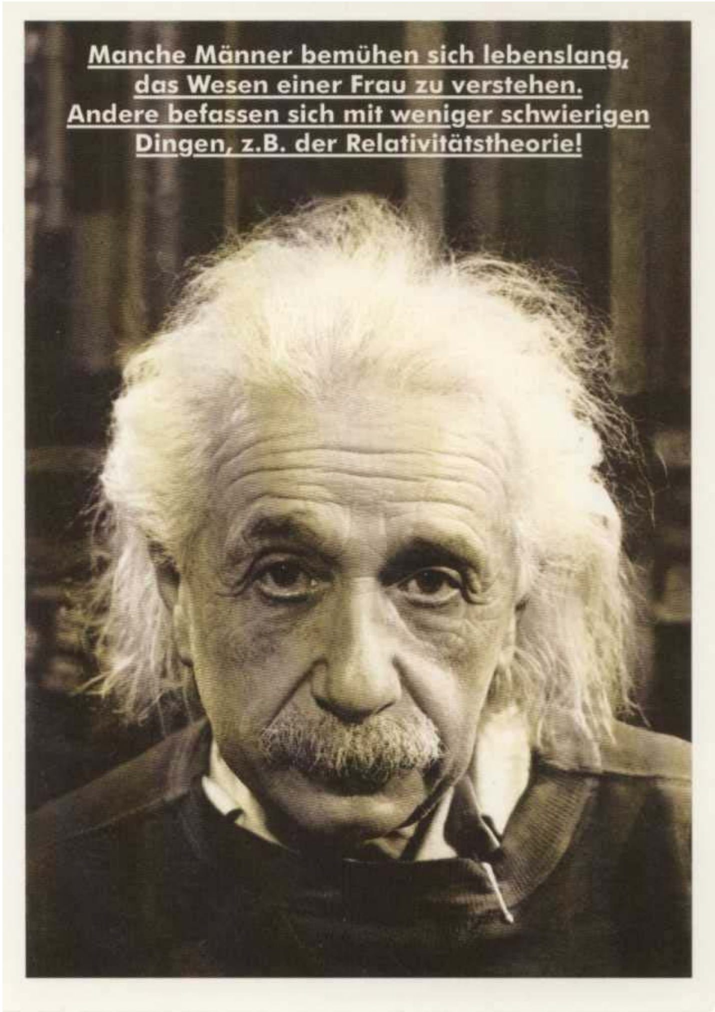

Figure 8: Last but not least ...